ISSN: 1410-8917
Jurnal Kimia Sains & Aplikasi
e-ISSN: 2597-9914

Jurnal Kimia Sains dan Aplikasi 29 (5) (2026): 314-327

Jurnal Kimia Sains dan Aplikasi
Journal of Scientific and Applied Chemistry

Journal homepage: http://ejournal.undip.ac.id/index.php/ksa

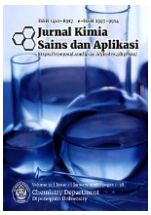

In Silico Study of Fatty Acid Compounds in Pure Eel Oil (*Anguilla marmorata* (Q.) Gaimard) as a Therapeutic Agent for Liver Cancer

Shara Wardhani, Saipul Maulana, Jamaluddin Jamaluddin *

Department of Pharmacy, Universitas Tadulako, Jl. Soekarno Hatta No.KM. 9, Tondo, Mantikulore, Palu 94148, Indonesia

* Corresponding author: jamal_farmasi02@yahoo.co.id

https://doi.org/10.14710/jksa.29.5.314-327

Article Info

Article history:

Received: 22nd January 2026
Revised: 10th May 2026
Accepted: 18th May 2026
Online: 15th June 2026

Keywords:
Liver cancer; Eel; network pharmacology; molecular docking; ADMET prediction

Abstract

Liver cancer is a leading cause of cancer-related deaths globally, due to late diagnosis and limited treatment options. Developing aquatic resources as sources of bioactive compounds with anti-inflammatory and antiproliferative activities may provide a potential strategy for exploring alternative therapeutic candidates for liver cancer. Eels (*Anguilla marmorata* (Q.) Gaimard) are known to contain fatty acids with anti-inflammatory and antiproliferative activities, potentially with anticancer activity. However, there have been no scientific reports related to specific fatty acid compounds in pure eel oil that have the potential to be liver anticancer agents. This study aims to identify the molecular targets of eel oil fatty acids with the potential to inhibit liver cancer cell growth and to analyze molecular interactions and binding affinities with target proteins. The methods used were an integrated computational approach of network pharmacology and molecular docking, accompanied by ADMET prediction. The results of this study showed that network pharmacology analysis predicted three main target proteins, namely SRC, PIK3CA, and PIK3CB, which play an important role in the pathogenesis of liver cancer. The molecular docking results showed that of the 34 eel compounds, six compounds showed strong binding affinity toward SRC, PIK3CA, and PIK3CB, such as 5,8,11,14,17-cis -Eicosapentaenoic Acid (SRC and PIK3CB), Eicosapentaenoic Acid (SRC), Cis-4,7,10,13,16,19 -Docosahexaenoic Acid (SRC, PIK3CA, and PIK3CB), Gamma-Linolenic Acid (PIK3CA), Arachidonic Acid (PIK3CA), and Cis 8,11,14-Eicosatrienoic Acid (PIK3CB). However, these docking scores were weaker than those of the native ligands (approximately -9 to -10 kcal/mol), suggesting relatively weak ATP-binding site occupancy compared with approved inhibitors. ADMET prediction suggested generally favorable ADME properties, and *in silico* toxicity predictions indicate low acute toxicity risk. In conclusion, this study identified fatty acid compounds from pure eel oil as multi-target therapeutic candidate compounds that may serve as preliminary multi-target candidate compounds for further experimental validation in liver cancer research.

1. Introduction

Liver cancer remains one of the leading causes of cancer-related death worldwide, and its global burden is projected to continue increasing in the coming decades [1, 2]. Among the various types of liver cancer, hepatocellular carcinoma (HCC) is the most common, accounting for approximately 90% of cases worldwide [3, 4]. HCC typically arises from malignant transformation of hepatocytes driven by chronic risk factors such as hepatitis B virus infection, hepatitis C virus infection, fatty liver disease, alcohol-related cirrhosis, smoking, obesity, diabetes, iron overload, and dietary exposures [5]. Current therapeutic strategies for HCC include surgical resection, liver transplantation, ablation, locoregional therapy, immunotherapy-based combinations, and molecularly targeted agents, including tyrosine kinase inhibitors. However, the prognosis remains consistently poor in many patients because HCC is frequently diagnosed at an advanced

stage, highlighting the need to explore novel therapeutic candidates [6, 7].

The diversity of aquatic resources represents a promising avenue for novel therapeutics, offering a rich reservoir of bioactive compounds with anticancer potential [8]. One example is the eel (*Anguilla marmorata* (Q.) Gaimard), which is abundant in Indonesia and has been reported to exhibit antihyperlipidemic, anti-inflammatory, anticancer, antibacterial, antifungal, antioxidant, and antiviral activities [9, 10]. The selection of *A. marmorata* as the primary subject of this study is based on its superior nutritional profile, particularly its high essential fatty acid content compared to other freshwater fish species.

Based on gas chromatography analysis, *A. marmorata* sourced from Lake Poso contains 22 fatty acid types, with oleic acid as the major component (40.01%–41.12%). It is further enriched with long-chain omega-3 fatty acids, specifically Eicosapentaenoic acid (EPA) at 0.85%–0.95% and Docosahexaenoic acid (DHA) at 5.45%–6.39% [11]. Previous studies on tropical Anguilla species have also reported that eel-derived oils and by-products are enriched with EPA and DHA, supporting their potential as sources of bioactive compounds for therapeutic development [12].

The presence of these bioactive compounds, known for their vital physiological functions in human health and cognitive function, provides a strong foundation for utilizing this species' chemical profile in targeted drug discovery. To explore this potential, computational approaches are well-suited to early-stage research, as they can substantially reduce time and cost before experimental validation. Network pharmacology can map relationships between these multiple compounds and various protein targets within disease-associated networks, while molecular docking predicts the binding affinities and modes of candidate compounds toward specific liver cancer targets [13].

Network pharmacology and molecular docking have been used to evaluate bioactive components against liver cancer in other studies, but have not been reported in eel oil [14]. To date, no scientific reports have specifically evaluated the anti-liver-cancer potential of the fatty acid compounds in pure eel oil using an integrated network pharmacology and molecular docking approach. Therefore, this study aimed to explore potential interactions between fatty acids from pure eel oil and liver cancer-related protein targets using an integrated network pharmacology and molecular docking approach. This *in silico* study was intended as a hypothesis-generating investigation to identify candidate compounds and molecular targets for future experimental validation.

2. Experimental

2.1. Tools and Materials

In this study, all computational analyses were performed on a computer equipped with an Intel® Core™ i5 processor and running Windows 10 Pro. The software utilized included Cytoscape 3.10.0 [15], AutoDock Tools version 1.5.7 [16], Discovery Studio Visualizer 20.1.0.19295 [17], and PyMOL 2.5.4 [18]. The materials used in this study were the three-dimensional structures of 34 fatty acid compounds contained in pure eel oil (*A. marmorata* (Q.) Gaimard) obtained from the list of compounds in the journal article about the fatty acid profile of pure eel oil [19].

The 3D crystal structure of selected target receptors obtained from the Protein Data Bank (PDB) (https://www.rcsb.org/). The molecular structures of eel compounds were represented using SMILES notation and retrieved from PubChem (https://pubchem.ncbi.nlm.nih.gov/, accessed on 2 July 2025), as shown in Table 1.

2.2. Identification of Targets Associated with Eel Compounds and Liver Cancer

To identify targets associated with eel's fatty acid compounds, the comprehensive SMILES notation, encompassing the various bioactive components of eel, was then used to query the SwissTargetPrediction (http://www.swisstargetprediction.ch/) [20], SEA (Similarity Ensemble Approach) database (https://sea.bkslab.org/) [21], BindingDB database (https://www.bindingdb.org/rwd/bind/index.jsp/) [22], and TargetNet database (http://targetnet.scbdd.com/calcnet/index_ensemble/) [23]. The prediction aimed to identify the most likely molecular targets associated with eel and its individual components. To identify targets associated with liver cancer, we accessed the DisGenet, Therapeutic Target Database, OMIM, Genecards, and Drugbank databases. The DisGenet (https://disgenet.com/) [24], Therapeutic Target Database (https://idrblab.net/ttd/) [25], Drugbank (https://go.drugbank.com/) [26], and Genecards (https://www.genecards.org/) databases [27], known for their comprehensive and user-friendly information on human genes, were utilized to gather data relevant to liver cancer.

Additionally, the OMIM database, which provides detailed information on genetic and hereditary diseases, was consulted (https://www.omim.org/) [28]. By searching for hepatocellular carcinoma in both databases, we identified key associated targets to this condition. Targets identified from these databases (non-redundant) were merged, and a Venn diagram was created using Venny 2.1.0 (https://bioinfogp.cnb.csic.es/tools/venny/) to illustrate the genes common to both eel compounds and liver cancer targets [29].

2.3. Protein–Protein Interaction (PPI) Network Construction

The common gene targets were uploaded to the STRING database (https://stringdb.org/) for analysis [30]. The species was set to Homo sapiens, confidence score of >0.9, and the resulting interaction network was then imported into Cytoscape 3.10.0 software. Statistical analysis was subsequently conducted based on degree values. The CytoCluster plugin was employed to identify the top 10 hub genes using the degree method [15].

Table 1. Fatty acid compounds of *A. marmorata* (Q.) Gaimard and their SMILES

No.	Compound	SMILES
1	Inhibitor AP23464 (native ligand)	-
2	Alpelisib (native ligand)	-
3	Pictilisib (native ligand)	-
4	Caprylic acid	CCCCCCCC(=O)O
5	Lauric acid	CCCCCCCCCCCC(=O)O
6	Tridecanoic acid	CCCCCCCCCCCCC(=O)O
7	Myristic acid	CCCCCCCCCCCCCC(=O)O
8	Pentadecanoic acid	CCCCCCCCCCCCCCC(=O)O
9	Palmitic acid	CCCCCCCCCCCCCCCC(=O)O
10	Heptadecenoic acid	CCCCCCC\C=C/CCCCCCCCCC(=O)O
11	Stearic acid	CCCCCCCCCCCCCCCCCC(=O)O
12	Arachidic acid	CCCCCCCCCCCCCCCCCCCC(=O)O
13	Henicosanoic acid	CCCCCCCCCCCCCCCCCCCCC(=O)O
14	Behenic acid	CCCCCCCCCCCCCCCCCCCCCC(=O)O
15	Lignoceric acid	CCCCCCCCCCCCCCCCCCCCCCCC(=O)O
16	Decanoic acid	CCCCCCCCCC(=O)O
17	Tricosanoic acid	CCCCCCCCCCCCCCCCCCCCCCC(=O)O
18	Myristoleic acid	CCCCC\C=C/CCCCCCCC(=O)O
19	Cis-10-palmitoleic acid	CCCCC\C=C/CCCCCCCCC(=O)O
20	Palmitoleic acid	CCCCCCC\C=C/CCCCCCCC(=O)O
21	Cis-10-heptadecenoic acid	CCCCCCC\C=C/CCCCCCCCCC(=O)O
22	Elaidic acid	CCCCCCCC/C=C\CCCCCCCC(=O)O
23	Oleic acid	CCCCCCCCC\C=C/CCCCCCCC(=O)O
24	5,8,11,14,17-cis-eicosapentaenoic acid	CCC=CCC=CCC=CCC=CC/C=C\CCCC(=O)O
25	Cis-11-eicosenoic acid	CCCCCCCCC\C=C/CCCCCCCCCC(=O)O
26	Erucic acid methyl ester	CCCCCCCCCCCC\C=C/CCCCCCCC(=O)OC
27	Butyric acid	CCCC(=O)O
28	Linolelaidic acid	CCCCCC/C=C\C/C=C\CCCCCCC(=O)O
29	Linoleic acid	CCCCCC\C=C/C\C=C/CCCCCCCC(=O)O
30	Gamma-linolenic acid	CCCCCC\C=C/C\C=C/C\C=C/CCCC(=O)O
31	Alpha-linolenic acid	CCC\C=C/C\C=C/C\C=C/CCCCCCCC(=O)O
32	Eicosadienoic acid	CCCCCC\C=C/C\C=C/CCCCCCCCCC(=O)O
33	Cis 8,11,14-eicosatrienoic acid	CCCCCC\C=C/C\C=C/C\C=C/CCCCCCC(=O)O
34	Eicosatrienoic acid methyl ester	CCC\C=C/C\C=C/C\C=C/CCCCCCCCCC(=O)OC
35	Arachidonic acid	CCCCC\C=C/C\C=C/C\C=C/C\C=C/CCC(=O)O
36	Eicosapentaenoic acid	CCC\C=C/C\C=C/C\C=C/C\C=C/C\C=C/CCCC(=O)O
37	Cis-4,7,10,13,16,19-docosahexaenoic acid	CCC\C=C/C\C=C/C\C=C/C\C=C/C\C=C/C\C=C/C(=O)O

2.4. Pathway and Functional Enrichment Analysis

The intersecting genes were evaluated via Gene Ontology (GO) and Kyoto Encyclopedia of Genes and Genomes (KEGG). We conducted GO functional annotation to categorize genes based on their biological roles, leveraging sequence similarity, experimental evidence, and the available literature. Additionally, the KEGG pathway analysis was employed to map out the complex interactions between genes, proteins, and small molecules within various biological contexts. For our study, we utilized the ShinyGo (http://bioinformatics.sdstate.edu/go74/) [31], WebGestalt (https://www.webgestalt.org/) [32] and the DAVID (https://davidbioinformatics.nih.gov/tools.jsp) database to conduct both GO functional annotation and KEGG pathway enrichment analyses [33]. Enrichment significance was evaluated using false discovery rate (FDR)-adjusted q-values, and the number of genes associated with each enriched term was recorded. The background gene set used for enrichment analysis consisted of Homo sapiens genes available in the respective databases.

2.5. Integrated Compound–Target–Pathway Network Construction

Significantly enriched KEGG pathways were used to map targets to pathways. The compound–target and target–pathway networks were imported into Cytoscape 3.10.0 and merged to form an integrated compound–target–pathway network; node identities were standardized. Redundant edges and isolated nodes were removed prior to visualization [34].

2.6. Molecular Docking Method Validation

Method validation was conducted by determining the grid box using AutoDock Tools v.1.5.6 and AutoDock Vina. The grid box dimensions were customized to the best binding pose. Molecular docking was validated until the root mean square deviation (RMSD) was less than 2 Å [35].

2.7. Molecular Docking and Visualization

Molecular docking was conducted using AutoDock Vina. Ligands were prepared in their predicted protonation states at physiological pH, and receptor preparation included removal of water molecules and non-essential co-crystallized ions prior to docking. Docking calculations were performed with an exhaustiveness value of 8 and num_modes of 9, using AutoDock Vina default settings. The prepared ligand and receptor structures were converted into .pdbqt format prior to docking analysis. The docking results were obtained as binding affinity scores and ligand–protein interaction conformations for further visualization and analysis [35].

2.8. ADMET Prediction

SMILES notation of potential eel compounds was submitted to the pkCSM (https://biosig.lab.uq.edu.au/) to predict ADME (absorption, distribution, metabolism, excretion) parameters, and to predict toxicity. The SMILES notation was submitted to the ProTox 3.0. (https://tox.charite.de/protox3/index.php/) [36].

3. Results and Discussion

3.1. Identification of Targets Associated with Eel Compounds and Liver Cancer

Potential eel-associated targets were identified through the SwissTargetPrediction database (409 genes), SEA (324 genes), BindingDB (41 genes), and TargetNet (581 genes). Liver cancer-associated targets were obtained from DisGeNET (703 genes), Therapeutic Target Database (57 genes), DrugBank (215 genes), GeneCards (9,924 genes), and OMIM (581 genes). We combined eel-associated genes and also liver cancer-associated genes. To visualize the overlap between the two combined genes, a Venn diagram was created. This analysis revealed 638 targets common to both eel and liver cancer, highlighting the potential for overlap between the two [34]. However, these shared targets were derived from integrated predictions across multiple ligand-based target prediction platforms and disease databases; therefore, the results should be interpreted cautiously as hypothesis-generating associations rather than experimentally validated targets.

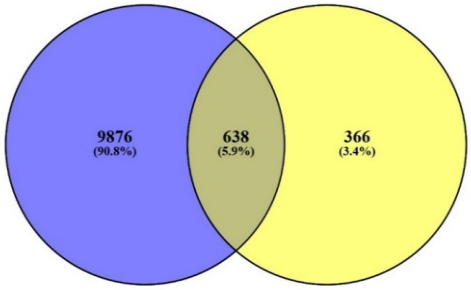

Figure 1. A Venn diagram shows the targets of eel compounds and liver cancer

The selection of the 34 fatty acids was based on the established chemical profile of *A. marmorata* oil [19]. It is important to note that the compounds identified as potent inhibitors, particularly EPA and DHA, are reported to be major constituents in this eel species [9, 10]. This high relative abundance ensures that the therapeutic potential observed in this *in silico* study is representative of the pure eel oil mixture rather than limited by trace isomers at negligible concentrations.

3.2. Protein–Protein Interaction (PPI) Network Construction

Analysis of the PPI network constructed from the overlapping eel-compound targets and liver cancer–associated genes revealed 546 nodes and 2,927 edges, with an average neighbor degree of 11,118, highlighting its complexity. The interaction degree of the targets is depicted by varying shades of color, as shown in Figure 2. Additionally, Figure 2 presents the top core liver cancer-related targets screened using degree values, with SRC, PIK3CA, and PIK3CB emerging as the targets with the highest degree values of 54, 52, and 48, respectively [37]. These findings are biologically plausible because SRC activation and PI3K pathway dysregulation are frequently associated with cancer progression and poor prognosis in HCC. However, PIK3CA in HCC should be interpreted primarily as a pathway-relevant target rather than a mutation-dominant driver, since reported mutation frequencies are generally low to moderate and cohort-dependent.

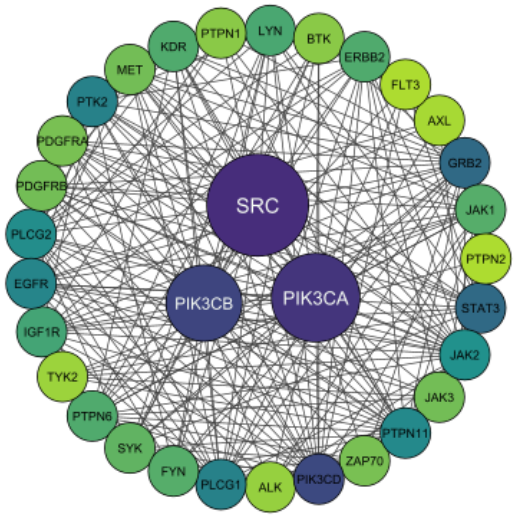

Figure 2. The network of top core liver cancer-related targets screened using degree values

3.3. Pathway and Functional Enrichment Analysis

For a detailed understanding of the key mechanisms involved in the action of eel-derived compounds against liver cancer, we conducted GO functional and KEGG enrichment annotation analyses for an in-depth gene annotation. The shinyGO KEGG dot plot is shown in Figure 3, where EGFR tyrosine-kinase inhibitor resistance ranked highest by fold enrichment, followed by non-small-cell lung cancer, VEGF signaling, ErbB/PD-1–PD-L1, JAK–STAT, HIF-1, Ras, focal adhesion, chemokine signaling, Rap1/PI3K–Akt, hepatitis B/EBV/KSHV infection, and proteoglycans in cancer [38].

The WebGestalt GO Biological Process summary is presented in Figure 4 section A, highlighting high counts for cell communication, metabolic process, response to stimulus, and biological regulation, with additional enrichment in multicellular organismal process, developmental process, localization, and cell population proliferation. Enriched Cellular Component categories are depicted in Figure 4, section B, clustering in the membrane and protein-containing complex, cytosol and nucleus, and the vesicle/endomembrane system, with contributions from the membrane-enclosed lumen, endosome, extracellular space, and cell projection/cytoskeleton. Molecular Function results are shown in Figure 4, section C, dominated by protein binding, ion binding, nucleotide binding, and transferase activity, followed by molecular transducer, enzyme regulator, and nucleic-acid binding [32].

Consistently, pathway-level mapping on Proteoglycans in cancer is illustrated in Figure 5, placing the eel-compound targets across SRC, PIK3CA, and PIK3CB that have the highest degree, highlighted modules converge on cell proliferation, survival, tumor cell migration, and invasion, in agreement with the enrichment patterns observed across shinyGO, WebGestalt, and DAVID [39].

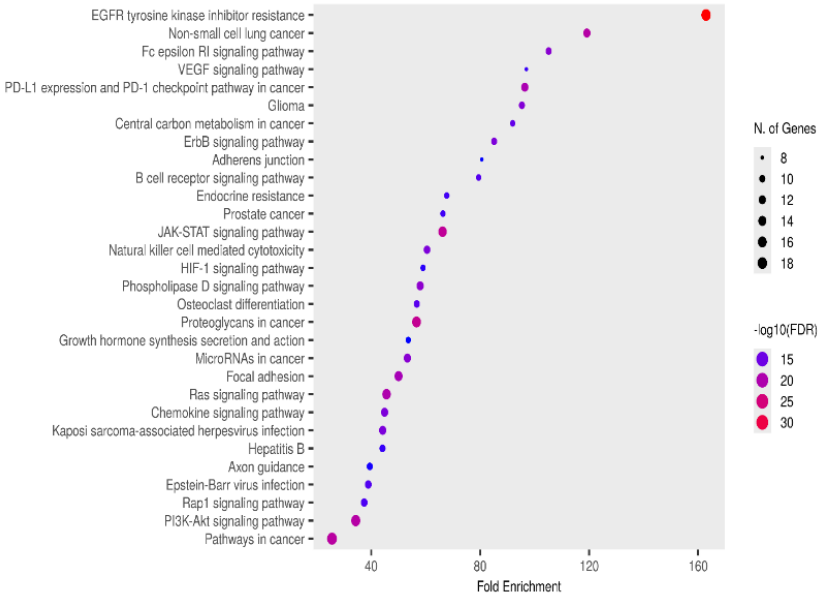

Figure 3. KEGG pathway enrichment (ShinyGO) for eel-compound targets. Dots show top pathways (size = overlap genes; color = significance)

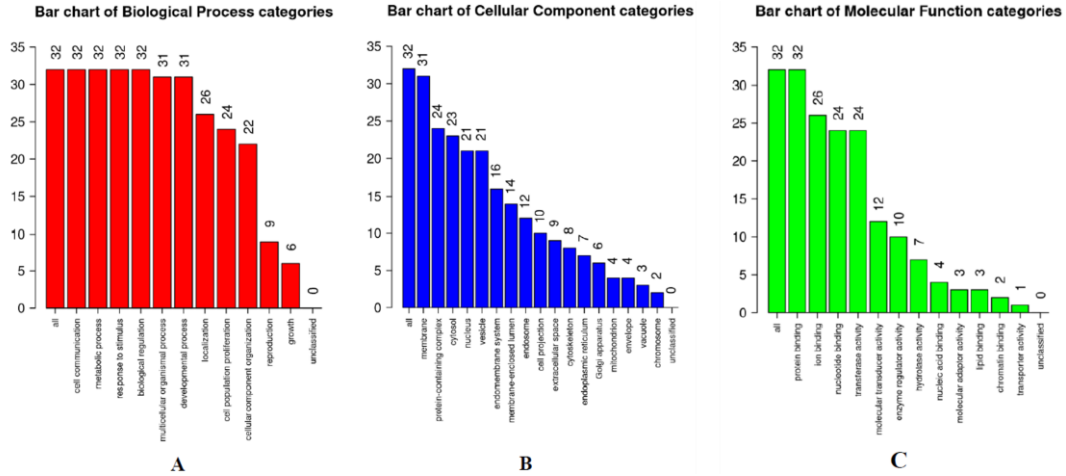

Figure 4. GO biological process enrichment (WebGestalt). Bars indicate the number of eel-compound target genes per term (A), gene counts per cellular compartment (B), and gene counts per molecular function (C)

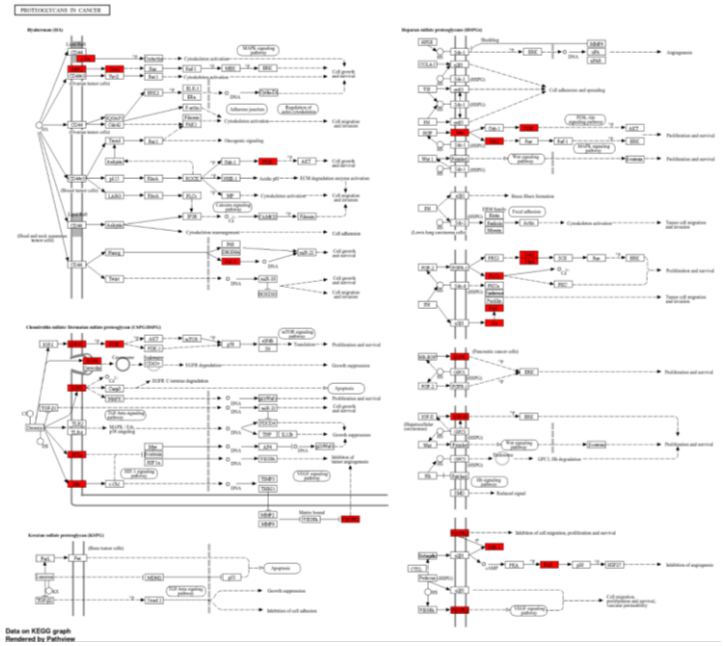

Figure 5. Diagram of pathways involving potential targets identified through KEGG analysis. The red sections highlight the eel compounds associated with liver cancer

3.4. Integrated Compound–Target–Pathway Network Construction

To explore the multi-target effects of the eel compound in liver cancer, two separate networks were constructed: the compound–target network and the target-pathway network. These two networks were subsequently merged to form an integrated compound–target-pathway network (Figure 6) [13, 40].

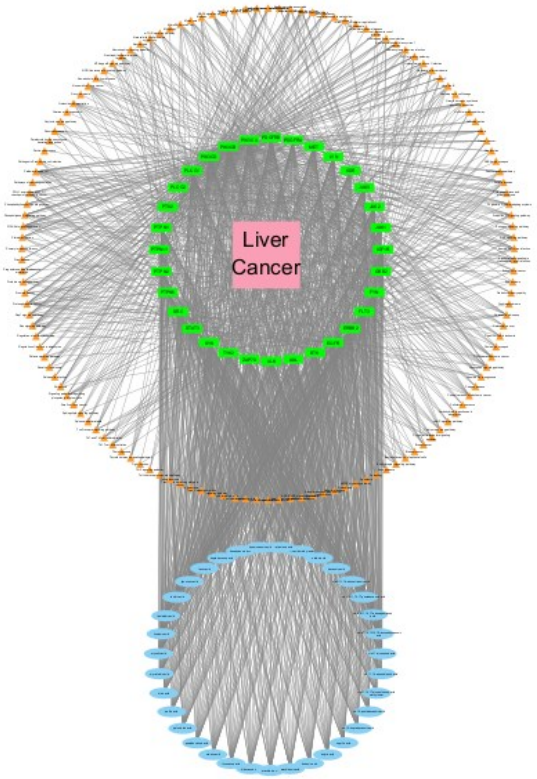

Figure 6. Compound–target–pathway network. The blue circles represent the fatty acid compounds of eel pure oil, the green rectangles represent the core genes, and the orange triangles represent the pathways linked to the core genes

3.5. Molecular Docking Method Validation

Validation was conducted to obtain a grid box that includes the active sites of the targets as binding targets by redocking the natural ligand to the targets. The targets used in this study were liver cancer-related proteins, namely SRC (PDB ID: 2BDJ; co-crystallized with AP23464), PIK3CA (PDB ID: 4JPS; co-crystallized with alpelisib), and PIK3CB (PDB ID: 2Y3A; co-crystallized with GDC-0941/pictilisib). The validation parameters are based on the RMSD, which indicates the degree of deviation of the ligand redocking results from the crystallographic ligands at the same binding site. The lower the RMSD value, the closer the ligand is to the native conformation, and this is considered a good position. The RMSD value is confirmed to be valid if it is less than or equal to 2 [16].

The validation results indicated that the optimal binding pose was located at the binding site coordinates x = 38, y = 20, and z = 28, with a grid box center at x = 13.988, y = -43.906, and z = 27.109 (Figure 7). The average RMSD obtained from 20 independent docking runs was below 2 Å. Since an RMSD value below 2 Å is generally accepted as a criterion for successful docking validation, the selected grid box configuration was considered valid and suitable for subsequent molecular docking studies of the test ligands [41].

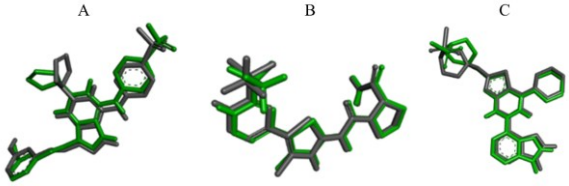

Figure 7. Validation of the ligand structure before (gray) and after docking (green) SRC (A) (RMSD = 1.259), PIK3CA (B) (RMSD = 0.893), and PIK3CB (C) (RMSD = 0.964)

3.6. Molecular Docking and Visualization

The results of molecular docking are presented as binding affinity values (Table 2). These values are key parameters in drug discovery that describe the strength of interactions between ligands and their targets, where lower values indicate stronger binding and greater complex stability [42]. For the SRC protein, 5,8,11,14,17-cis-eicosapentaenoic acid (-6.7 kcal/mol), gamma-linolenic acid (-6.5 kcal/mol), and cis-4,7,10,13,16,19-docosahexaenoic acid (-7.0 kcal/mol) showed favorable binding affinities. Ligand–protein interaction analysis revealed interactions with residues GLU A:310, GLY A:344, GLY A:274, ILE A:336, MET A:314, PHE A:405, SER A:345, and VAL A:323 through van der Waals forces, MET A:341 through hydrogen bonding, and VAL A:281 through alkyl interactions (Figure 8). Furthermore, the active site of SRC is located in the ATP-binding pocket, which includes key residues such as LYS A:295, GLU A:310, ASP A:404, MET A:341, THR A:338, TYR A:340, LEU A:393, GLY A:344, and SER A:345. These residues form several important active sites in the ATP-binding pocket, namely the hinge region (MET A:341), the ribose-binding pocket (GLY A:274, VAL A:281), and the hydrophobic pocket (LEU A:273, ALA A:293, MET A:314, ILE A:336, THR A:338, TYR A:340, LEU A:393). Interactions at these active sites are generally hydrophobic interactions [42].

Table 2. Docking results of fatty acid compounds of the eel

No.	Compound	Binding affinity (kkal/mol)		
		SRC	PIK3CA	PIK3CB
1	Inhibitor AP23464 (native ligand)	**-10.3**	-	-
2	Alpelisib (native ligand)	-	**-10.4**	-
3	Pictilisib (native ligand)	-	-	**-9.3**
4	Caprylic acid	-5.0	-5.3	-5.0
5	Lauric acid	-5.4	-5.0	-5.4
6	Tridecanoic acid	-5.3	-5.3	-5.6
7	Myristic acid	-5.5	-5.4	-5.5
8	Pentadecanoic acid	-5.6	-6.3	-5.4
9	Palmitic acid	-5.4	-5.4	-5.7
10	Heptadecenoic acid	-5.7	-5.3	-6.3
11	Stearic acid	-5.7	-4.9	-5.5
12	Arachidic acid	-5.8	-5.1	-5.4
13	Henicosanoic acid	-5.6	-5.2	-5.5
14	Behenic acid	-5.7	-5.5	-5.8
15	Lignoceric acid	-5.7	-5.4	-5.4
16	Decanoic acid	-5.3	-5.4	-5.6
17	Tricosanoic acid	-5.6	-5.9	-5.4
18	Myristoleic acid	-5.6	-5.6	-5.8
19	Cis-10-palmitoleic acid	-5.8	-5.3	-5.9
20	Palmitoleic acid	-5.8	-5.8	-5.7
21	Cis-10-heptadecenoic acid	-5.8	-5.6	-5.8
22	Elaidic acid	-3.9	-4.1	-4.2
23	Oleic acid	-6.0	-5.3	-5.8
24	5,8,11,14,17-cis-eicosapentaenoic acid	**-6.7**	-6.0	-6.3
25	Cis-11-eicosenoic acid	-5.7	-5.8	-5.9
26	Erucic acid methyl ester	-5.9	-5.7	-4.8
27	Butyric acid	-3.9	-4.7	-4.2
28	Linolelaidic acid	-6.0	-5.9	-5.9
29	Linoleic acid	-6.1	-5.8	-6.5
30	Gamma-linolenic acid	**-6.5**	**-6.4**	**-6.5**
31	Alpha-linolenic acid	-6.0	-5.9	-6.0
32	Eicosadienoic acid	-5.8	-6.2	-6.1
33	Cis 8,11,14-eicosatrienoic acid	-6.2	-6.3	**-7.0**
34	Eicosatrienoic acid methyl ester	-5.9	-5.9	-5.7
35	Arachidonic acid	-6.2	**-6.8**	-6.2
36	Eicosapentaenoic acid	-6.4	-5.5	-5.5
37	Cis-4,7,10,13,16,19-docosahexaenoic acid	**-7.0**	**-7.0**	**-6.9**

In the test ligand, interactions were observed in amino acids GLU A:310, GLY A:344, and SER A:345 primarily through hydrophobic and van der Waals interactions within the ATP-binding pocket, while limited interactions were observed near MET A:341 in the hinge region. These interaction patterns suggest relatively weak, non-specific occupancy of the lipophilic ATP-binding pocket compared with that of the native ligand. The binding of fatty acid compounds to the ATP-binding pocket of SRC, particularly through interactions with the hinge region (MET A:341), prevents the autophosphorylation of the Tyr416 residue, which is essential for SRC activation. This molecular blockade triggers a downstream cascade that inhibits liver cancer proliferation through the identified pathways.

In the VEGF signaling pathway, inhibiting SRC reduces VEGF expression and prevents FAK/paxillin activation, which are critical for the angiogenic and proliferative responses of HCC cells. Simultaneously, in the Rap1 signaling pathway, suppressing SRC activity prevents activation of RapGEFs, thereby attenuating the Ras/MAPK signaling axis that typically drives uncontrolled cell cycle progression. Consequently, the interaction of these eel-derived fatty acids with the SRC ATP-binding pocket serves as a molecular switch to downregulate these key signaling modules, ultimately halting tumor cell growth. This is in accordance with a study conducted on the molecular docking of fatty acid compounds to the SRC protein. The results of this study show that fatty acids occupy the ATP-binding pocket and interact mainly through hydrophobic forces in the form of van der Waals, Figure 8. The interaction of the native ligand, potential eel oil compound, and SRC alkyl, and π- alkyl with nonpolar residues in the hydrophobic pocket of SRC [40].

In the PIK3CA protein, gamma-linolenic acid (-6.4 kcal/mol), arachidonic acid (-6.8 kcal/mol), and cis-4,7,10,13,16,19-docosahexaenoic acid (-7.0 kcal/mol) compounds have good binding affinity values. Analysis of ligand–protein interactions shows that ligands interact with several residues around the ATP-binding pocket. Residues ARG A:852, ASN A:853, ASP A:933, PHE A:930, and MET A:772 interact through van der Waals forces, while SER A:854 and VAL A:851 form conventional hydrogen bonds, and HIS A:855 and VAL A:850 interact through alkyl forces (Figure 9). The active site of PIK3CA is located in the ATP-binding pocket, which includes key residues such as VAL A:851, which acts as a hydrogen bond anchor in the hinge region, GLN A:859, which determines PI3Kα selectivity through reciprocal hydrogen bonds, and the aromatic residues TYR A:836 and TRP A:780, which contribute to $\pi-\pi$ interactions.

In addition, LYS A:802 is involved in water-mediated electrostatic networks, while ASP A:933 from the DFG motif functions as a hydrogen bond donor/acceptor at the edge of the catalytic pocket. The residues ILE A:848, ILE A:800, ILE A:932, MET A:772, and PRO A:778 play a role in forming a hydrophobic pocket in the ATP pocket [43]. In the test ligand, interactions are seen with the amino acids VAL A:851, ASP A:933, and MET A:772 through hydrophobic interactions. This indicates that the test ligand occupies the ATP-binding pocket with an interaction pattern consistent with the key residues of PIK3CA. This is consistent with another study, which found that ligands occupy the PIK3CA ATP-binding pocket and interact primarily through hydrophobic forces in the form of van der Waals, alkyl, and π–alkyl interactions with nonpolar residues in the hydrophobic pocket, reinforced by hydrogen bonds in the hinge region [44].

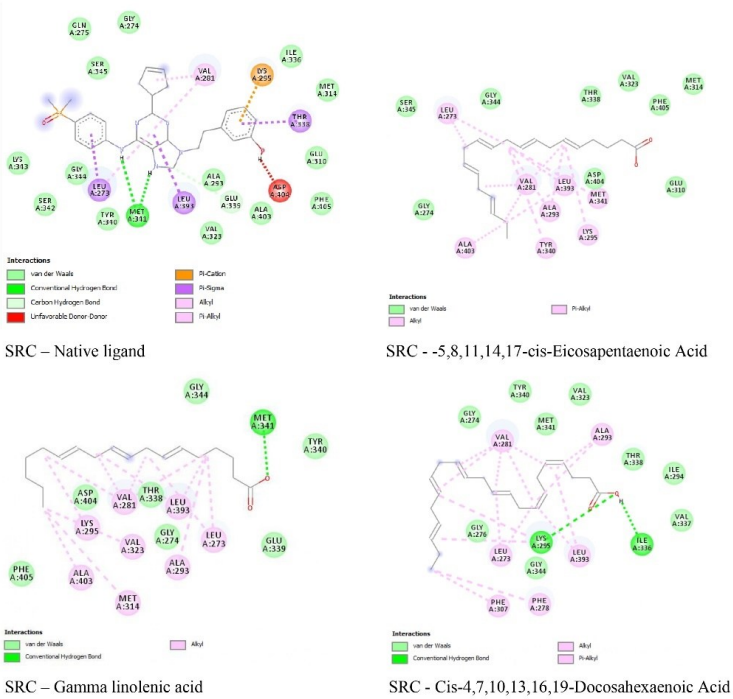

Figure 8. The interaction of the native ligand, potential eel oil compound, and SRC

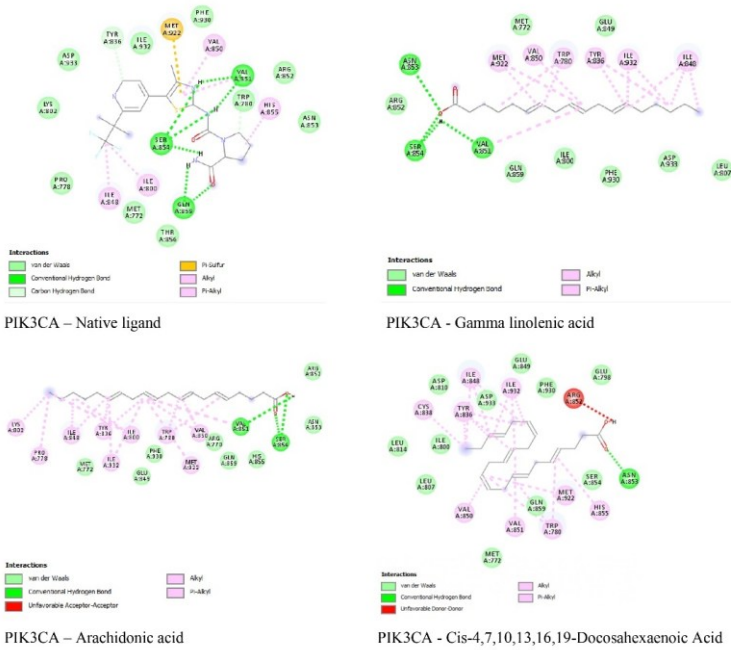

Figure 9. The interaction of the native ligand, potential eel oil compound, and PIK3CA

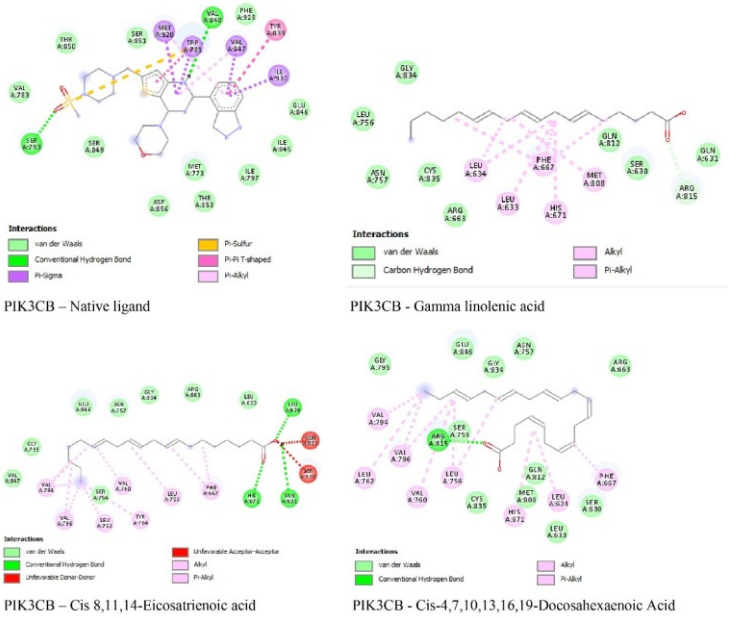

Figure 10. The interaction of the native ligand, potential eel oil compound, and PIK3CB

The PIK3CB protein also showed promising interactions with gamma-linolenic acid (-6.5 kcal/mol), cis-8,11,14-eicosatrienoic acid (-7.0 kcal/mol), and cis-4,7,10,13,16,19-docosahexaenoic acid (-6.9 kcal/mol), which have fairly good binding affinity values. Analysis of ligand–protein interactions shows that all GLU A:846 residues interact with the ligand through van der Waals forces (Figure 10). In the active site of PIK3CB, there are potential hydrogen bonds at TYR A:677 and SER A:1046, as well as steric collisions between the protrusions at ALA A:674, PRO A:676, and GLU A:675. Generally, the type of interaction between the ligand and PIK3CB is hydrophobic [45]. The docking results suggest that the fatty acid ligands occupy the ATP-binding and hydrophobic pockets of PIK3CB, interacting primarily with GLU A:846 through van der Waals and hydrophobic interactions. These findings are consistent with the reported role of PIK3CB in regulating fatty acid metabolism and histone acetylation in cancer [46].

Although the binding affinities of the fatty acids (-3.9 to -7.0 kcal/mol) were clearly weaker than those of the native ligands/inhibitors (-9.3 to -10.4 kcal/mol), these values may still indicate moderate binding and potential target engagement rather than strong inhibitory potency, because molecular docking scores in this range can still reflect energetically favorable ligand–protein interactions, especially when the compounds occupy the same binding pocket as the reference ligands and maintain contacts with key active-site residues. Accordingly, docking scores should be interpreted alongside binding mode analysis rather than as direct measures of pharmacological potency.

Table 3. ADMET prediction results from pkCSM and ProTox (Compound 1 = 5,8,11,14,17-cis-eicosapentaenoic acid; compound 2 = gamma-linolenic acid; compound 3 = cis-4,7,10,13,16,19-docosahexaenoic acid; compound 4 = arachidonic acid; compound 5 = cis 8,11,14-eicosatrienoic acid)

Category	Parameters	Reference	Compound				
			1	2	3	4	5
Absorption	Water solubility (log mol/L)	> -6	-5.976	-5.787	-6.024	-5.897	-6.17
	Caco-2 permeability (log Papp in 10^{-6} cm/s)	> 0.9	1.588	1.577	1.594	1.583	1.574
	Intestinal absorption (human) (%)	> 30%	93.16	92.83	93.32	92.99	91.80
	Skin permeability (log Kp)	> -2.5	-2.727	-2.722	-2.729	-2.725	-2.731
	P-glycoprotein substrate	No	No	No	No	No	No
	P-glycoprotein I inhibitor	No	No	No	No	No	No
	P-glycoprotein II inhibitor	No	No	No	No	No	No
Distribution	VDss (human) (log L/kg)	< -0.15	-0.671	-0.617	-0.702	-0.643	-0.623
	Fraction unbound (human)	< 0.1	0.021	0.056	0.009	0.037	0.009
	BBB permeability	> -1	-0.145	-0.115	-0.161	-0.13	-0.241
	CNS permeability (log PS)	> -2	-1.331	-1.547	-1.224	-1.439	-1.383
Metabolism	CYP2D6 substrate	No	No	No	No	No	No
	CYP3A4 substrate	No	Yes	Yes	Yes	Yes	Yes
	CYP1A2 inhibitor	No	Yes	Yes	Yes	Yes	Yes
	CYP2C19 inhibitor	No	No	No	No	No	No
	CYP2C9 inhibitor	No	No	No	No	No	No
	CYP2D6 inhibitor	No	No	No	No	No	No
	CYP3A4 inhibitor	No	No	Yes	No	No	No
Excretion	Total clearance (log mL/ min/kg)	> 0	2.155	1.99	2.269	2.072	2.084
	Renal OCT2 substrate	No	No	No	No	No	No
Toxicity	LD_{50} (mg/kg)	> 2000	10000	10000	10000	10000	10000
	Toxicity class	> 5	6	6	6	6	6

Therefore, the present docking results should not be interpreted as direct evidence of biological efficacy. Instead, their relevance lies in the observation that several fatty acids occupied the ATP-binding pocket and shared interaction patterns with key active-site residues of SRC, PIK3CA, and PIK3CB, suggesting functionally meaningful binding [39, 47, 48]. Taken together, these findings support the view that eel oil fatty acids may serve as preliminary multi-target lead compounds, but their actual anticancer activity must be confirmed through further in vitro and in vivo studies, including enzyme inhibition and cell-based antiproliferative assays.

Visualization of the molecular docking results shows that van der Waals interactions, conventional hydrogen bonds, and alkyl interactions occur between the ligands and amino acid residues at the active site of the target protein. However, it is important to note that the binding affinity values of the fatty acid compounds (-6.0 to -7.0 kcal/mol) are significantly weaker compared to the native ligands (-9.3 to -10.4 kcal/mol), which represents a multi-fold difference in binding strength on a logarithmic scale. Although these results indicate substantially weaker binding affinity than that of optimized synthetic inhibitors, they may still provide weak docking support for potential biological activity. In addition, potential allosteric or membrane-modulatory effects of these fatty acids cannot be excluded. Test ligands that interact with the same amino acid residues on the active site of the target protein, such as the hinge region (MET A:341 in SRC) and the ATP-binding pocket, may still contribute to therapeutic effects through natural multi-target synergy [49].

In previous studies, a similar pattern was observed: natural compounds exhibited lower affinity than reference drugs but retained high functional relevance through interactions with key catalytic residues. Thus, while these fatty acids are not as potent as the controls, their ability to occupy the same active site supports their potential as naturally derived alternative agents [50]. Overall, the docking results suggest relatively low target selectivity, as many saturated and unsaturated fatty acids showed similar binding affinities across SRC, PIK3CA, and PIK3CB. Given that SRC, PIK3CA, and PIK3CB play important roles in tumor cell proliferation, survival, migration, and invasion, which contribute to liver cancer, these compounds are expected to reduce liver cancer progression by suppressing the excessive activity of these three targets.

Furthermore, the simultaneous interaction of various fatty acids with these interconnected targets suggests a strong multi-target synergistic effect. This synergy likely compensates for the lower individual binding affinities of the fatty acids compared to the native ligands. By cumulatively disrupting multiple critical nodes within the liver cancer signaling network, the combined presence of these fatty acids in pure eel oil enhances its overall potential as an effective multi-target therapeutic agent.

Compounds with lower binding affinity than the native ligand are still considered to possess significant biological potential due to their ability to interact specifically with key amino acid residues at the active site, such as MET A:341 in SRC or VAL A:851 in PIK3CA, thereby mimicking essential interaction patterns required to inhibit the target protein function. This indicates that biological efficacy is not solely determined by binding affinity but also by the precision of interactions within the binding pocket, such as the formation of specific hydrogen bonds with particular residues, which may trigger strong cytotoxicity.

In addition, interactions across different regions of the protein may regulate the activity of these compounds, resulting in specific biological effects in certain cell types. The tested compounds exhibited stable binding patterns, adopting orientations highly similar to those of the native ligand. This phenomenon is consistent with previous reports in which two Schizandrin derivatives retained biological activity despite differences in binding affinity, as both compounds bound in the same orientation as the native ligand and replicated interactions with key residues within the active pocket [51].

ADMET predictions (Table 3) indicate that 5,8,11,14,17-cis-eicosapentaenoic acid, gamma-linolenic acid, cis-4,7,10,13,16,19-docosahexaenoic acid, arachidonic acid, and cis-8,11,14-eicosatrienoic acid exhibit high gastrointestinal absorption, with Caco-2 permeability values above the pkCSM threshold of 0.9 log Papp (10^{-6} cm/s), based on pkCSM prediction criteria. However, the water solubility of these compounds varies, which may affect their oral bioavailability, indicating the need for the development of special formulations to increase their solubility. Nevertheless, these compounds were not predicted to be P-gp substrates by pkCSM under default settings, which may contribute to their systemic bioavailability. All of these compounds also have low skin absorption, requiring special formulations to produce topical preparations. In addition, the low unbound fraction values suggest high plasma protein binding, consistent with the albumin-binding properties of long-chain fatty acids.

The predicted BBB permeability and CNS permeability values suggest limited to moderate central nervous system exposure; therefore, these predictions should be interpreted cautiously. In terms of metabolism, these compounds largely do not interfere with the metabolism of other drugs, so the potential for drug interactions when used with other drugs is lower. In terms of excretion, all compounds show similar renal clearance in the range of 1.9-2.3 log mL/min/kg, and none are substrates for the OCT2 transporter, indicating that excretion is not dependent on renal transporters. The toxicity profile shows that all compounds are safe, except for the toxicity results for cis-4,7,10,13,16,19-docosahexaenoic acid, which is hazardous if ingested and therefore requires a special formulation to ensure safety for oral administration. The oral toxicity analysis confirms that the major fatty acids in eel oil, particularly DHA, exhibit very high LD_{50} values (10,000 mg/kg). This suggests a favorable safety profile for further development as a therapeutic agent for liver cancer [52].

Overall, the results of this study suggest that the fatty acid content of pure eel oil may have potential as a source of bioactive compounds for liver cancer research. Previous preclinical studies have reported that omega-3 fatty acids such as EPA and DHA may suppress HCC cell proliferation and promote apoptosis; however, clinical translation remains limited, and these compounds are not currently recommended in HCC treatment guidelines as anticancer therapies. This potential provides opportunities for the development of liver cancer therapies based on natural ingredients, especially from aquatic resources such as eels, which can be an alternative to existing therapy options.

4. Conclusion

Protein targets with the gene names SRC, PIK3CA, and PIK3CB, which are associated with the fatty acid compounds in pure eel oil (*Anguilla marmorata* (Q.) Gaimard), are involved in the pathogenesis of liver cancer. The fatty acid compounds in pure eel oil have the potential to inhibit liver cancer target proteins against SRC target proteins, namely 5,8,11,14,17-cis-eicosapentaenoic acid, gamma-linolenic acid, and cis-4,7,10,13,16,19-docosahexaenoic acid; against PIK3CA, namely gamma-linolenic acid, arachidonic acid, and cis-4,7,10,13,16,19-docosahexaenoic acid; and on PIK3CB, namely gamma-linolenic acid, cis-8,11,14-eicosatrienoic acid, and cis-4,7,10,13,16,19-docosahexaenoic acid. In conclusion, this study suggests that fatty acids from *Anguilla marmorata* may interact with key liver cancer targets, specifically SRC, PIK3CA, and PIK3CB. However, docking scores are substantially weaker than those of native ligands, and predominantly hydrophobic interactions suggest relatively low affinity and non-selective engagement of the ATP-binding site. Furthermore, the computational ADMET profiles indicated high plasma protein binding, limited water solubility, and predicted low acute toxicity, which should be interpreted cautiously. Therefore, these compounds may serve as preliminary structural scaffolds for further drug optimization and require extensive in vitro and in vivo validation to confirm their therapeutic potential against liver cancer.

References

[1] H. Sung, J. Ferlay, R. L. Siegel, M. Laversanne, I. Soerjomataram, A. Jemal, F. Bray, Global Cancer Statistics 2020: GLOBOCAN Estimates of Incidence and Mortality Worldwide for 36 Cancers in 185 Countries, *CA: A Cancer Journal for Clinicians*, 71, 3, (2021), 209-249 https://doi.org/10.3322/caac.21660

[2] Harriet Rumgay, Melina Arnold, Jacques Ferlay, Olufunmilayo Lesi, Citadel J. Cabasag, Jérôme Vignat, Mathieu Laversanne, Katherine A. McGlynn, Isabelle Soerjomataram, Global burden of primary liver cancer in 2020 and predictions to 2040, *Journal of Hepatology*, 77, 6, (2022), 1598-1606 https://doi.org/10.1016/j.jhep.2022.08.021

[3] Josep M. Llovet, Robin Kate Kelley, Augusto Villanueva, Amit G. Singal, Eli Pikarsky, Sasan Roayaie, Riccardo Lencioni, Kazuhiko Koike, Jessica Zucman-Rossi, Richard S. Finn, Hepatocellular carcinoma, *Nature Reviews Disease Primers*, 7, (2021), 6 https://doi.org/10.1038/s41572-020-00240-3

[4] A. Villanueva, Hepatocellular Carcinoma, *New England Journal of Medicine*, 380, (2019), 1450-1462 https://doi.org/10.1056/NEJMra1713263

[5] Ju Dong Yang, Pierre Hainaut, Gregory J. Gores, Amina Amadou, Amelie Plymoth, Lewis R. Roberts, A global view of hepatocellular carcinoma: trends, risk, prevention and management, *Nature Reviews Gastroenterology & Hepatology*, 16, (2019), 589-604 http://dx.doi.org/10.1038/s41575-019-0186-y

[6] David Anwanwan, Santosh Kumar Singh, Shriti Singh, Varma Saikam, Rajesh Singh, Challenges in liver cancer and possible treatment approaches, *Biochimica et Biophysica Acta - Reviews on Cancer*, 1873, 1, (2020), 188314 https://doi.org/10.1016/j.bbcan.2019.188314

[7] Melissa M. Center, Ahmedin Jemal, International Trends in Liver Cancer Incidence Rates, *Cancer Epidemiology, Biomarkers & Prevention*, 20, 11, (2011), 2362-2368 https://doi.org/10.1158/1055-9965.EPI-11-0643

[8] Nagaraju Bandaru, Yash Pramod Patil, Sumit Dilip Ekghara, Kunal Sharad Patil, Mohan Gandhi Bonthu, Exploring marine-derived compounds as potential anticancer agents: Mechanisms and therapeutic implications, *Cancer Pathogenesis and Therapy*, 4, 3, (2025), 192-207 https://doi.org/10.1016/j.cpt.2025.08.004

[9] Hanina Dzikrina, Siti Awalia Nur Fadillah, Shintya Yuniar, Wahyu Surakusumah, Diah Kusumawaty, Trina Ekawati Tallei, Evaluation of in silico anti-inflammatory potential of bioactive compound in *Anguilla bicolor*, *AIP Conference Proceedings*, 2694, 1, (2023), 030001 https://doi.org/10.1063/5.0119233

[10] Fea Prihapsara, Anif Nur Artanti, Melati Sekar Hasna Hanun, Salsabila Nanda Fatiha, Fadhilla Nur Cahyani, Sholichah Rohmani, Karakterisasi Nanoemulsi Minyak Tulang Ikan Sidat dengan Ekstrak Daun Salam dan Uji Aktivitas Antihiperlipidemia, *ALCHEMY Jurnal Penelitian Kimia*, 19, 1, (2023), 14-22 https://doi.org/10.20961/alchemy.19.1.61169.14-22

[11] Jamaluddin, Ayu Putu Putriasih, Yonelian Yuyun, Agustinus Widodo, The Comparison Extraction Methods of Crude Fat Content and Fatty Acid Profile of Eels (*Anguilla marmorata* (Q.) Gaimard) from Lake Poso, *Journal of Pharmacy and Nutrition Sciences*, 9, 2, (2019), 119-124 https://doi.org/10.29169/1927-5951.2019.09.02.11

[12] L. Gómez-Limia, N. Cobas, I. Franco, S. Martínez-Suárez, Fatty acid profiles and lipid quality indices in canned European eels: Effects of processing steps, filling medium and storage, *Food Research International*, 136, (2020), 109601 https://doi.org/10.1016/j.foodres.2020.109601

[13] S. Yuan, B. Zuo, S. C. Zhou, M. Wang, K. Y. Tan, Z. W. Chen, W. F. Cao, Integrating Network Pharmacology and Experimental Validation to Explore the Pharmacological Mechanism of Astragaloside IV in Treating Bleomycin-Induced Pulmonary Fibrosis, *Drug Design, Development and Therapy*, 17, (2023), 1289-1302 http://dx.doi.org/10.2147/DDDT.S404710

[14] Songyan Tie, T. Tong, G. Zhan, X. Li, D. Ouyang, J. Cao, Network pharmacology prediction and

experiment validation of anti-liver cancer activity of *Curcumae rhizoma* and *Hedyotis diffusa Willd*, *Annals of Medicine and Surgery*, 86, 6, (2024), 3337-3348 https://doi.org/10.1097/ms9.0000000000002074

[15] Paul Shannon, Andrew Markiel, Owen Ozier, Nitin S. Baliga, Jonathan T. Wang, Daniel Ramage, Nada Amin, Benno Schwikowski, Trey Ideker, Cytoscape: A Software Environment for Integrated Models of Biomolecular Interaction Networks, *Genome Research*, 13, 11, (2003), 2498-2504 https://doi.org/10.1101/gr.1239303

[16] G. M. Morris, R. Huey, W. Lindstrom, M. F. Sanner, R. K. Belew, D. S. Goodsell, A. J. Olson, AutoDock4 and AutoDockTools4: Automated docking with selective receptor flexibility, *Journal of Computational Chemistry*, 30, (2009), 2785-2791 https://doi.org/10.1002/jcc.21256

[17] BIOVIA Discovery Studio, Discovery Studio Visualizer 2020, (2020),

[18] L. Schrödinger, The PyMOL Molecular Graphics System, (2021),

[19] Jamaluddin, Yuliet, Wa Ode S. Musnina, Yonelian Yuyun, Syahna Shaldan, S. Malasugi, Putri A. Arta, Gina N. Putri, Adetya Maryani, Muhammad F. Haq, Syamsul Lakahoro, Nurul Awwaliyah P. Firman, Siti B. Al-Amri, Sinta Amelia, Asriani Hasanuddin, Novalina Serdiati, Jusri Nilawati, The Effect of Adsorbents on the Quality of Refined Eel Fish (*Anguilla marmorata* [Q.] Gaimard) Oil as a Raw Material for Pharmaceutical Preparations, *Jurnal Penelitian Pendidikan IPA*, 10, 12, (2024), 10759-10792 https://doi.org/10.29303/jppipa.v10i12.9806

[20] Antoine Daina, Olivier Michielin, Vincent Zoete, SwissTargetPrediction: updated data and new features for efficient prediction of protein targets of small molecules, *Nucleic Acids Research*, 47, W1, (2019), W357-W364 https://doi.org/10.1093/nar/gkz382

[21] Michael J. Keiser, Bryan L. Roth, Blaine N. Armbruster, Paul Ernsberger, John J. Irwin, Brian K. Shoichet, Relating protein pharmacology by ligand chemistry, *Nature Biotechnology*, 25, (2007), 197-206 https://doi.org/10.1038/nbt1284

[22] Michael K. Gilson, Tiqing Liu, Michael Baitaluk, George Nicola, Linda Hwang, Jenny Chong, BindingDB in 2015: A public database for medicinal chemistry, computational chemistry and systems pharmacology, *Nucleic Acids Research*, 44, D1, (2016), D1045-D1053 https://doi.org/10.1093/nar/gkv1072

[23] Z. J. Yao, J. Dong, Y. J. Che, M. F. Zhu, M. Wen, N. N. Wang, S. Wang, A. P. Lu, D. S. Cao, TargetNet: a web service for predicting potential drug–target interaction profiling via multi-target SAR models, *Journal of Computer-Aided Molecular Design*, 30, (2016), 413-424 http://dx.doi.org/10.1007/s10822-016-9915-2

[24] Janet Piñero, Juan Manuel Ramírez-Anguita, Josep Saüch-Pitarch, Francesco Ronzano, Emilio Centeno, Ferran Sanz, Laura I. Furlong, The DisGeNET knowledge platform for disease genomics: 2019 update, *Nucleic Acids Research*, 48, D1, (2019), D845–D855 https://doi.org/10.1093/nar/gkz1021

[25] Yunxia Wang, Song Zhang, Fengcheng Li, Ying Zhou, Ying Zhang, Zhengwen Wang, Runyuan Zhang, Jiang Zhu, Yuxiang Ren, Ying Tan, Chu Qin, Yinghong Li, Xiaoxu Li, Yuzong Chen, Feng Zhu, Therapeutic target database 2020: enriched resource for facilitating research and early development of targeted therapeutics, *Nucleic Acids Research*, 48, D1, (2019), D1031–D1041 https://doi.org/10.1093/nar/gkz981

[26] David S. Wishart, Yannick D. Feunang, An C. Guo, Elvis J. Lo, Ana Marcu, Jason R. Grant, Tanvir Sajed, Daniel Johnson, Carin Li, Zinat Sayeeda, Nazanin Assempour, Ithayavani Iynkkaran, Yifeng Liu, Adam Maciejewski, Nicola Gale, Alex Wilson, Lucy Chin, Ryan Cummings, Diana Le, Allison Pon, Craig Knox, Michael Wilson, DrugBank 5.0: a major update to the DrugBank database for 2018, *Nucleic Acids Research*, 46, (2018), D1074-D1082 https://doi.org/10.1093/nar/gkx1037

[27] G. Stelzer, N. Rosen, I. Plaschkes, S. Zimmerman, M. Twik, S. Fishilevich, T. I. Stein, R. Nudel, I. Lieder, Y. Mazor, S. Kaplan, D. Dahary, D. Warshawsky, Y. Guan-Golan, A. Kohn, N. Rappaport, M. Safran, D. Lancet, The GeneCards Suite: From Gene Data Mining to Disease Genome Sequence Analyses, *Current Protocols in Bioinformatics*, 54, 1, (2016), 1.30.31-31.30.33 https://doi.org/10.1002/cpbi.5

[28] Joanna S. Amberger, Carol A. Bocchini, Alan F. Scott, Ada Hamosh, OMIM.org: leveraging knowledge across phenotype–gene relationships, *Nucleic Acids Research*, 47, D1, (2019), D1038-D1043 https://doi.org/10.1093/nar/gky1151

[29] J. C. Oliveros, Venny. An Interactive Tool for Comparing Lists with Venn's Diagrams, *Bioinformatics*, (2007),

[30] Damian Szklarczyk, Rebecca Kirsch, Mikaela Koutrouli, Katerina Nastou, Farrokh Mehryary, Radja Hachilif, Annika L. Gable, Tao Fang, Nadezhda T. Doncheva, Sampo Pyysalo, Peer Bork, Lars J. Jensen, Christian von Mering, The STRING database in 2023: protein-protein association networks and functional enrichment analyses for any sequenced genome of interest, *Nucleic Acids Research*, 51, D1, (2023), D638-D646 https://doi.org/10.1093/nar/gkac1000

[31] Steven Xijin Ge, Dongmin Jung, Runan Yao, ShinyGO: a graphical gene-set enrichment tool for animals and plants, *Bioinformatics*, 36, 8, (2020), 2628-2629 https://doi.org/10.1093/bioinformatics/btz931

[32] Yuxing Liao, Jing Wang, Eric J. Jaehnig, Zhiao Shi, Bing Zhang, WebGestalt 2019: gene set analysis toolkit with revamped UIs and APIs, *Nucleic Acids Research*, 47, W1, (2019), W199-W205 https://doi.org/10.1093/nar/gkz401

[33] Brad T. Sherman, Ming Hao, Ju Qiu, Xiaoli Jiao, Michael W. Baseler, H. Clifford Lane, Tomozumi Imamichi, Weizhong Chang, DAVID: a web server for functional enrichment analysis and functional annotation of gene lists (2021 update), *Nucleic Acids Research*, 50, W1, (2022), W216-W221 https://doi.org/10.1093/nar/gkac194

[34] Gui-biao Zhang, Qing-ya Li, Qi-long Chen, Shi-bing Su, Network Pharmacology: A New Approach for Chinese Herbal Medicine Research, *Evidence-Based Complementary and Alternative Medicine*, 2013, (2013), 621423 http://dx.doi.org/10.1155/2013/621423

[35] Jerome Eberhardt, Diogo Santos-Martins, Andreas F. Tillack, Stefano Forli, AutoDock Vina 1.2.0: New Docking Methods, Expanded Force Field, and Python Bindings, *Journal of Chemical Information and Modeling*, 61, 8, (2021), 3891-3898 https://doi.org/10.1021/acs.jcim.1c00203

[36] Douglas E. V. Pires, Tom L. Blundell, David B. Ascher, pkCSM: Predicting Small-Molecule Pharmacokinetic and Toxicity Properties Using Graph-Based Signatures, *Journal of Medicinal Chemistry*, 58, 9, (2015), 4066−4072 https://doi.org/10.1021/acs.jmedchem.5b00104

[37] Chia-Hao Chin, Shu-Hwa Chen, Hsin-Hung Wu, Chin-Wen Ho, Ming-Tat Ko, Chung-Yen Lin, *cytoHubba*: identifying hub objects and sub-networks from complex interactome, *BMC Systems Biology*, 8, (2014), S11 https://doi.org/10.1186/1752-0509-8-S4-S11

[38] Steven Xijin Ge, Dongmin Jung, Runan Yao, ShinyGO: a graphical gene-set enrichment tool for animals and plants, *Bioinformatics*, 36, 8, (2018), 2628−2629 https://doi.org/10.1093/bioinformatics/btz931

[39] Ouided Benslama, Sabrina Lekmine, Hamza Moussa, Hichem Tahraoui, Mohammad Shamsul Ola, Jie Zhang, Abdeltif Amrane, Silymarin as a Therapeutic Agent for Hepatocellular Carcinoma: A Multi-Approach Computational Study, *Metabolites*, 15, 1, (2025), 53 https://doi.org/10.3390/metabo15010053

[40] J. M. Guzmán-Flores, V. Pérez-Vázquez, F. Martínez-Esquivias, M. A. Isiordia-Espinoza, J. M. Viveros-Paredes, Molecular Docking Integrated with Network Pharmacology Explores the Therapeutic Mechanism of *Cannabis sativa* against Type 2 Diabetes, *Current Issues in Molecular Biology*, 45, 9, (2023), 7228-7241 https://doi.org/10.3390/cimb45090457

[41] Hidayatul Lailiyyah, Lisa Lisdiana, Uji Aktivitas Antibakteri Senyawa Aktif Temu Kunci (*Boesenbergia rotunda*) terhadap *Mycobacterium tuberculosis* secara *In Silico LenteraBio*, 12, 2, (2023), 132-149

[42] Danislav S. Spassov, Binding Affinity Determination in Drug Design: Insights from Lock and Key, Induced Fit, Conformational Selection, and Inhibitor Trapping Models, *International Journal of Molecular Sciences*, 25, 13, (2024), 7124 https://doi.org/10.3390/ijms25137124

[43] Pascal Furet, Vito Guagnano, Robin A. Fairhurst, Patricia Imbach-Weese, Ian Bruce, Mark Knapp, Christine Fritsch, Francesca Blasco, Joachim Blanz, Reiner Aichholz, Jacques Hamon, Doriano Fabbro, Giorgio Caravatti, Discovery of NVP-BYL719 a potent and selective phosphatidylinositol-3 kinase alpha inhibitor selected for clinical evaluation, *Bioorganic & Medicinal Chemistry Letters*, 23, 13, (2013), 3741-3748 https://doi.org/10.1016/j.bmcl.2013.05.007

[44] Md. Rezaul Karim, Md. Niaj Morshed, Safia Iqbal, Shahnawaz Mohammad, Ramya Mathiyalagan, Deok Chun Yang, Yeon Ju Kim, Joon Hyun Song, Dong Uk Yang, A Network Pharmacology and Molecular-Docking-Based Approach to Identify the Probable Targets of Short-Chain Fatty-Acid-Producing Microbial Metabolites against Kidney Cancer and Inflammation, *Biomolecules*, 13, 11, (2023), 1678 https://doi.org/10.3390/biom13111678

[45] X. Zhang, O. Vadas, O. Perisic, K. E. Anderson, J. Clark, P. T. Hawkins, L. R. Stephens, R. L. Williams, Structure of Lipid Kinase p110β/p85β Elucidates an Unusual SH2-Domain-Mediated Inhibitory Mechanism, *Molecular Cell*, 41, 5, (2011), 567-578 http://dx.doi.org/10.1016/j.molcel.2011.01.026

[46] Yixin Duan, Juanjuan Liu, Jianxin Xu, Jing Fang, PI3Kβ moonlights as a protein kinase: driving fatty acid metabolism and histone acetylation in cancer, *Cancer Biology & Medicine*, 22, (2025), 20250216 https://doi.org/10.20892/j.issn.2095-3941.2025.0216

[47] Nikos Koundouros, Evdoxia Karali, Aurelien Tripp, Adamo Valle, Paolo Inglese, Nicholas J. S. Perry, David J. Magee, Sara Anjomani Virmouni, George A. Elder, Adam L. Tyson, Maria Luisa Dória, Antoinette van Weverwijk, Renata F. Soares, Clare M. Isacke, Jeremy K. Nicholson, Robert C. Glen, Zoltan Takats, George Poulogiannis, Metabolic Fingerprinting Links Oncogenic *PIK3CA* with Enhanced Arachidonic Acid-Derived Eicosanoids, *Cell*, 181, 7, (2020), 1596-1611.e1527 https://doi.org/10.1016/j.cell.2020.05.053

[48] Fan Wu, Zheng Zhao, Rui-Chao Chai, Yu-Qing Liu, Guan-Zhang Li, Hao-Yu Jiang, Tao Jiang, Prognostic power of a lipid metabolism gene panel for diffuse gliomas, *Journal of Cellular and Molecular Medicine*, 23, 11, (2019), 7741-7748 https://doi.org/10.1111/jcmm.14647

[49] C. Shivanika, S. Deepak Kumar, V. Ragunathan, P. Tiwari, A. Sumitha, P. Brindha Devi, Molecular docking, validation, dynamics simulations, and pharmacokinetic prediction of natural compounds against the SARS-CoV-2 main-protease, *Journal of Biomolecular Structure and Dynamics*, 40, 2, (2022), 585-611 https://doi.org/10.1080/07391102.2020.1815584

[50] Juni Ekowati, Bimo Ario Tejo, Saipul Maulana, Wisnu Ananta Kusuma, Rizka Fatriani, Nabila Sekar Ramadhanti, Norhayati Norhayati, Kholis Amalia Nofianti, Melanny Ika Sulistyowaty, Muhammad Sulaiman Zubair, Takayasu Yamauchi, Iwan Sahrial Hamid, Potential Utilization of Phenolic Acid Compounds as Anti-Inflammatory Agents through TNF-α Convertase Inhibition Mechanisms: A Network Pharmacology, Docking, and Molecular Dynamics Approach, *ACS Omega*, 8, 49, (2023), 46851-46868 https://doi.org/10.1021/acsomega.3c06450

[51] G. Dileep Kumar, B. Siva, K. Bharathi, A. Devi, P. Pavan Kumar, K. Anusha, Surbhi Lambhate, T. Karunakar, Ashok Kumar Tiwari, K. Suresh Babu, Synthesis and biological evaluation of Schizandrin derivatives as tubulin polymerization inhibitors, *Bioorganic & Medicinal Chemistry Letters*, 30, 16, (2020), 127354 https://doi.org/10.1016/j.bmcl.2020.127354

[52] Nagwa M. Abdelazeem, Wael M. Aboulthana, Ashraf S. Hassan, Abdulrahman A. Almehizia, Ahmed M. Naglah, Hamad M. Alkahtani, Synthesis, *in silico* ADMET prediction analysis, and pharmacological evaluation of sulfonamide derivatives tethered with pyrazole or pyridine as anti-diabetic and anti-Alzheimer's agents, *Saudi Pharmaceutical Journal*, 32, 5, (2024), 102025 https://doi.org/10.1016/j.jsps.2024.102025